

A STUDY OF METHODS TO INCREASE
THE LIFT OF SUPERSONIC AIRFOILS AT LOW SPEEDS

Thesis
by

Lt. Comdr. A. D. Pollock, Jr., U.S.N.
and
Lt. Comdr. F. F. Reck, U.S.N.

In Partial Fulfillment of the Requirements for the
Professional Degree
in Aeronautical Engineering

California Institute of Technology
Pasadena, California

1947

ACKNOWLEDGEMENTS

The authors wish to express their appreciation to Mr. H. T. Nagamatsu for his interest in the problem and his many helpful suggestions.

Special thanks is to be given to Dr. E. E. Sechler, Mr. W. H. Bowen, and members of the GALCIT staff for their assistance and advice in making the experimental installation and final preparation of the data and pictures.

Appreciation and gratitude are expressed to Mr. Peter Kyropolis for his unfailing generosity with equipment under his cognizance.

TABLE OF CONTENTS

	Page
Acknowledgements	i
Table of Contents	ii
Notations	iii
Table of Figures	iv
Summary	v
I. DISCUSSION OF PROBLEM	
Discussion	1
II. EXPERIMENTAL PROCEDURE	
A. Discription of the Models	5
B. Corrections of Measurements	7
C. Procedure	7
a. Part I Model I	8
b. Part II Model II	9
D. Computation	10
III. RESULTS AND CONCLUSIONS	
A. Results	13
B. Conclusions	14
References	16

NOTATIONS

b	Model span
c	Model chord
C_D	Drag coefficient
C_{D_T}	Tare drag coefficient
C_{D_P}	Parasite drag coefficient
C_L	Lift coefficient
$C_{M_{25}}$	Moment coefficient about 25% chord
$C_{M_{50}}$	Moment coefficient about 50% chord
C_Q	Volumetric coefficient
d	Tare drag
D	Drag
L	Lift
m	Tare moment
M	Moment
P_o	Static pressure in model
q	Dynamic pressure in tunnel
Q	Quantity of air (corrected)
Q_R	Quantity of air (Rotameter)
R	gas constant
T	Temperature of air in model
v_s	Velocity of jet at slit
V	Tunnel velocity
γ	Ratio of specific heat

TABLE OF FIGURES

Figure

- 1 Drawing of Model II
- 2 Schematic air system diagram
- 3 Tuft survey pictures, no flap
- 4 Tuft survey pictures, 60° trailing edge flap
- 5 Tuft survey pictures, 15° nose flaps
- 6 Tuft survey pictures, combination flaps
- 7 Total head survey $\alpha = 6^\circ$
- 8 Total head survey $\alpha = 10^\circ$
- 9 Total head survey $\alpha = 14^\circ$
- 10 Model I - Wing polar at positive and negative increments of α .
No flaps
- 11 Comparison of $C_{L_{\max}}$ and C_D with various nose or trailing flap de-
flection - Model I
- 12 Comparison of $C_{L_{\max}}$ and C_D with combinations of nose and trailing
edge flaps - Model I
- 13 Model II - Comparison of $C_{L_{\max}}$ and C_D with various flap configurations
- 14 Variation $C_{L_{\max}}$ and $C_{D_{\max}}$ with variation of P_o
- 15 Model II - Polar with various P_o (No flaps)
- 16 Model I - Polar various trailing edge flaps
- 17 Model I - Polar various nose flaps
- 18 Model I - Polar various configurations of combined flaps
- 19 Model II - Polar trailing edge flaps $C_q = .0070$
- 20 Model II - Polar various configurations of combined flaps
- 21 Table I - Comparison of Results
- 22 Table II - Comparison of Results

SUMMARY

This thesis presents a study of the problem of improving the lift characteristics of a supersonic wing at low speeds. Trailing edge split flaps, nose flaps, and boundary layer control were investigated singularly and together using the optimum configuration of each.

Results indicate that the nose flap has an appreciable effect on preventing separation and thus increasing the lift. Split flaps give an increment of lift as would be expected. The boundary layer control consisted of blowing a sheet of high velocity air back over the top surface of the wing with very definite improvements of the lift and drag characteristics.

The work on the blowing technique, it is suggested, indicates sufficient promise to warrant much further study. The relatively large increment of lift that can be attributed to the prevention of flow separation at high angles of attack suggests that such boundary layer control could be used to improve controllability and to delay the stall, particularly tip stall, of high speed aircraft with very large sweep back angles.

I. DISCUSSION OF PROBLEM

Currently the double circular arc or wedge airfoils have shown considerable promise for high speed airplanes. These symmetrical wing sections are characterized by sharp leading and trailing edges necessary for flight at the higher Mach numbers. The shape and the sharpness of the airfoils, however, affect the maximum lift in an undesirable manner at low speeds. Consequently, as the wing loading is increased by structural requirements, fuel and power plant weight, etc., the problem of maximum lift of the high speed sections has become more important particularly with respect to landing and low speed flight.

The lift characteristics of high speed airfoils could be improved, it was felt, by trailing edge flaps, nose flaps, and by boundary layer control, along with still other means. From existing data, it appears that the increment of increased lift that one could expect from trailing flaps was not enough to reduce the landing speed of a supersonic airplane sufficiently. The use of boundary layer, although much unrelated experimental data exists, (see table of references) as a means of increasing the lift and reducing the drag of wedge or circular arc airfoils has not been fully exploited. At least the reports of such work are not available. The Germans have investigated the nose flap and it appears to show considerable promise in delaying separation, thus being effective in air maneuvers as well as in low speed flight.

The use of boundary layer control as a means of improving the flight qualities of an airplane has in the past not been generally

practicable. The aircraft reciprocating engine has not been particularly adaptable to such an installation to say nothing of the weight considerations, structural difficulties, or ducting complications. Also, the requirement of a great jump in the lift increment has not been sufficient to warrant solution of the aforementioned problems. With the advent of the jet power plants has come the requirement that the r.p.m. not be reduced below a certain minimum value in order to maintain the fire in the burners. Consequently, the pilot of the current jet planes is handicapped in landing since considerable power must be maintained in order to assure that he can take a wave off if necessary. This problem is acute in the carrier landing. The use of boundary layer control on the jet airplane where necessary is felt to be feasible since the power and the pump are available. The axial flow turbine type engine could accommodate a boundary layer blowing system nicely. The turbine compressor while supplying air to the boundary control blowing system would necessarily have to be operated at a relatively high r.p.m. to maintain enough air flow to the burning chamber. This type of system would provide a higher lift coefficient, less axial thrust, and would permit greater acceleration of the airplane since the power is more readily available.

The existing data on boundary layer studies, although not directly applicable to this thesis, seem to indicate that suction of the boundary layer is more effective than blowing. However, it should be pointed out that it is more difficult to maintain negative pressure than positive pressure. Most of the available

reports deal with boundary layer control or improvement on low speed conventional section wings or wing flap combinations and almost all use low pressure systems.

W. Schwier at Goettingen (ref. 1) has done considerable work on the blowing technique. Using an NACA 23012-64 airfoil and blowing air out immediately ahead of the flaps and immediately behind the hinged nose, he reports the following results:

Plain flaps, deflection = 45°

No air blown, $C_Q = 0$ $C_{L_{max}} = 2.18$

 at $C_Q = .020$ $C_{L_{max}} = 3.70$

Corresponding values for slotted flap

No air blown, $C_Q = 0$ $C_{L_{max}} = 2.38$

$C_Q = .020$ $C_{L_{max}} = 4.0$

Using a 9% wing (ref. 2) with a slot-flap and a slat he reports:

With open slat, deflected flap

No air blown $C_Q = 0$ $C_L = 1.86$

 at $C_Q = .025$ $C_L = 3.5$

The nose flap (ref. 3) used with a high-speed section has shown considerable increase of the maximum lift. The effect of this high-lift device can be explained by the fact that at a suitable deflection angle the front stagnation point of the flow will be displaced quite near the leading edge of this flap. This effect diminishes the considerable super velocities observed near the leading edge of the high speed profile at high angles of attack. Thus the steep pressure rise behind the leading edge is reduced and the stalling is delayed

to higher angles of attack. The stalling characteristics of high speed profiles with nose flaps become similar to those of normal leading edge radius.

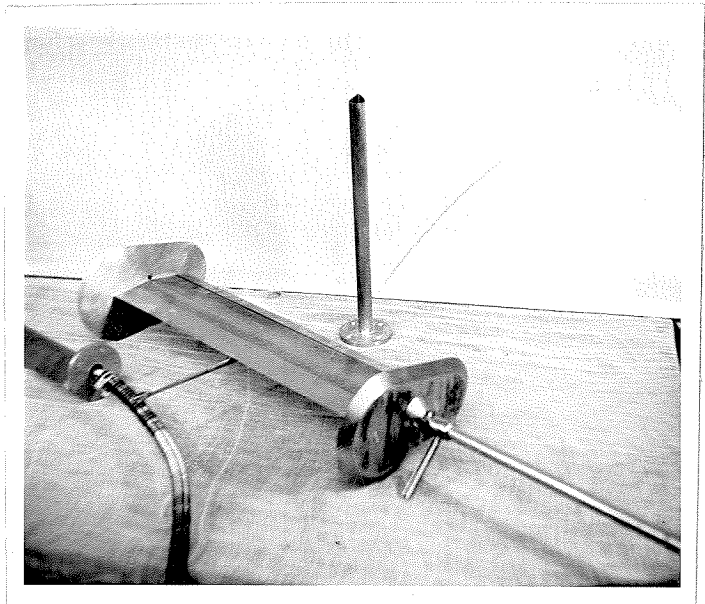
II. EXPERIMENTAL PROCEDURE

A. Description of the models

Two similar models were used in the experiments. The basic design of the models was a ten percent thick, symmetrical double-wedge section wing with a five inch chord and a twenty inch span. End plates were used to give a higher aspect ratio.

Model I, made of laminated wood with 0.10 inch end plates was used for the preliminary survey.

Model II was made of 0.10 inch phosphor bronze plates soldered or screwed to the ribs and end plates (Fig. 1). The model's surface was sealed except at the slit. Air was taken into the model through both end supports and blown out over the top surface from the span-wise slit which was located at the 15% chord line.



Model II showing support tube, fairing, and flexible hose.

It was necessary to put 0.005 inch shims at 1-1/2 inch stations across the span to maintain a uniform slit opening. The model was designed to withstand sufficient internal pressure so that a Mach number of one could be reached in the slit. This feature assured an even spanwise distribution of flow across the model.

The air was conducted into the model (Fig. 2) in the tunnel through pipes attached rigidly to the end plates. These pipes were used as the model support pivots and were shielded by externally

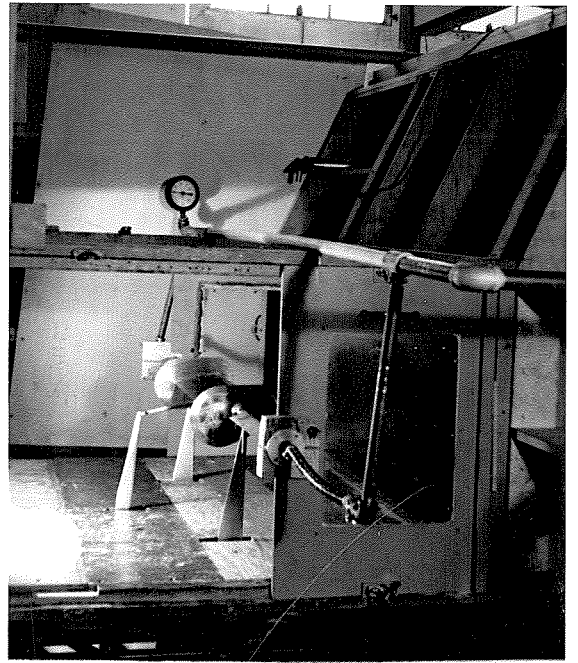
attached fairings. Soft rubber hoses enclosed in a find wire coil spring, of sufficient length to prevent external forces from being transmitted to the model, were attached to the outboard ends of the support pipes.

Air was piped to both sides of the tunnel through a settling tank to reduce the oil vapor content. Downstream from the tank a Rotameter flow gage was used to measure the quantity of flow.

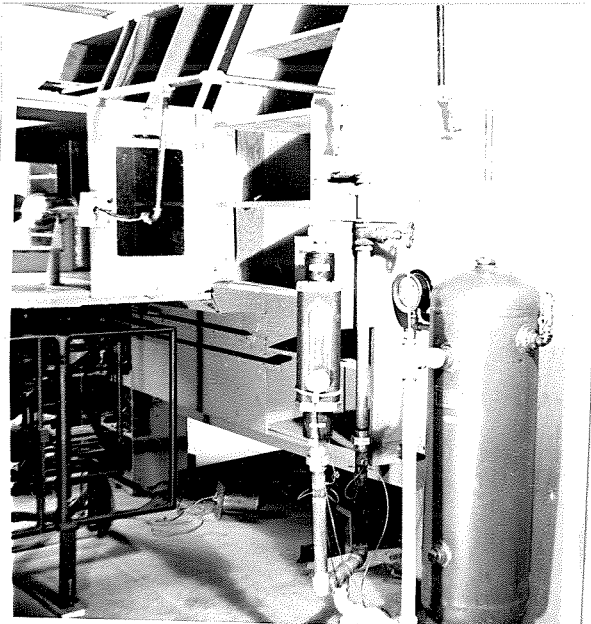
Pressure taps were provided at four stations spanwise across the model. Pressure gages were located on the tank, at the Rotometer, and at a point just outside of the tunnel.

Temperature of the air was measured between the tank and the flow meter by means of a thermometer set in a tee pipe coupling.

Split training edge flaps of 25% chord length with 15, 30, 45, 60, and 70, degree deflection and nose flaps of 10% chord length with 90, 120, 135, 150, and 180 degree deflections were provided. The flaps were attached to the model with screws and scotch tape.



Piping to the Model



Rotameter, settling tank thermometer and pressure gage installation.

B. Corrections of Measurements

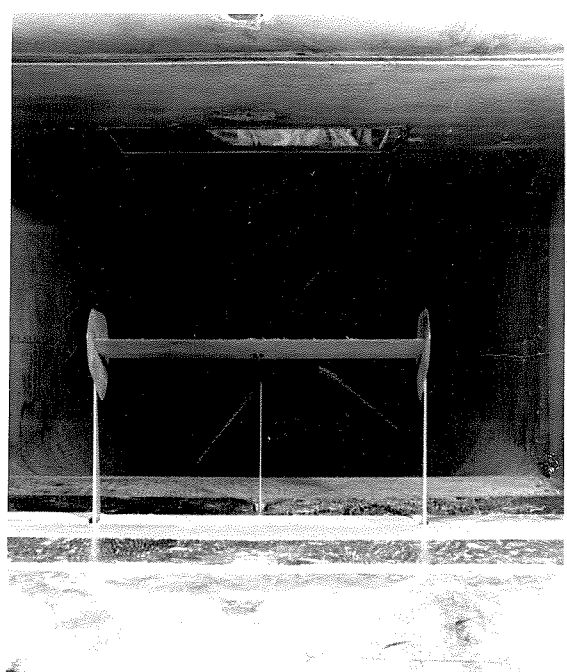
The drag correction for Model I was ascertained by using the image system method. Since Model II was essentially the same as Model I except for the end plates and the slit, the drag correction was determined by making similar runs and comparing the data. It was assumed that the difference in the drag at various angles of attack was due to the end plates and model support interference, and the air connection fittings on the end plates which were not faired. The drag correction obtained in this way turned out, within the limits of accuracy, to be a constant for all angles of attack.

Tare moment correction runs were made with both models. In order to duplicate operating conditions with Model II the air line between the flexible hose connection and the model was blocked and 44.7 psi absolute pressure was maintained in the line.

C. Procedure

The experiment was carried out at the C.I.T.-Merrill (24 x 48 inch) wind tunnel located at the Pasadena Junior College.

The usual work was divided essentially into two parts in order to minimize delays. The first part consisted of preliminary work with Model I during the period that Model II was being constructed. Model I was used, with good success, to investigate the boundary layer separation; the most promising flap configurations and combinations.



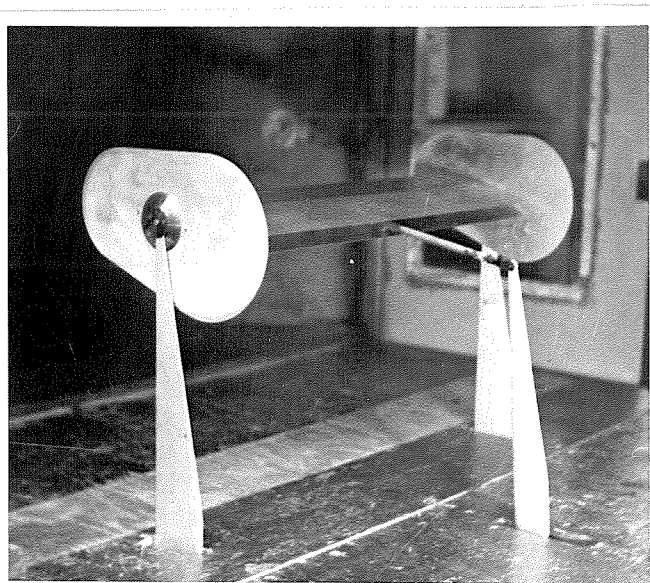
Front view of Model I installed in PJC Merrill tunnel for tuft survey

and the basic corrections and polars for the experiment. In the second part Model II was used to check the optimum configurations as found in Part I. The effect of boundary control on these configurations was investigated.

a) Part I (Model I)

A tuft survey (Figs. 3 to 6) and a total head pressure investigation (Figs. 7 to 9) was conducted in order to approximate the slit position on Model II. These surveys clearly indicate that separation of the flow began at the sharp leading edge and progressed aft as the angle of attack was increased. It was decided therefore, to locate the slit on Model II as far forward as possible. Due to the shape of the model and internal clearance requirements, the slit was located at the 15% chord line.

Complete runs measuring lift, drag and pitching moment were made with Model I. The first runs were made without flaps at both positive and negative increments of angle of attack (Fig. 10) in order to get the basic curves for comparative purposes. A series of runs were made using trailing edge flaps only (Fig. 16) and comparison of the data indicated that the 60° flap configuration was the optimum. Runs were made using the various nose flaps showing 150° deflection to be the optimum (Fig. 11). The runs of combined flaps were started using a trailing flap deflection and a nose flap



Model I installation 30°
trailing edge flaps

deflection of 60 and 150 degrees respectively. The flap configuration was varied to check the best combinations (Fig. 12)

b) Part II (Model II)

A complete run without flaps or blowing was made with Model II to compare the basic lift, drag and pitching moment with Model I. The wing without flap but with air blowing from the slit was run at 24.7, 34.7 and 44.7 psi absolute pressure. Since it was apparent (Fig. 15) that the 44.7 psi pressure gave the best relative results this pressure was used in all the succeeding blowing runs. As could be expected, C_Q at the various pressures used, had little variation. At 44.7, 34.7, 24.7 psi absolute the values of the discharge coefficient (C_Q) were 0.0070, 0.0064, and 0.00634 respectively. Deformation of the slit opening and structural consideration prevented tests at higher internal pressures.

Separate runs were made with trailing edge flaps (Fig. 19) and nose flaps at $C_Q = 0.0070$ to check the optimum separate flap deflections as indicated by Model I. Then runs were made with both flaps installed. Various combinations of the flaps were investigated to find the optimum configuration (Fig. 20).

During the runs when air was being blown from the model slit the pressure at the Rotameter was maintained constant and continuous readings of the air temperature and the quantity of flow were recorded. The pressure in the model was read at four stations and was found to be constant. Since the lines from the model to the Rotameter were relatively short and the diameters of the lines were large compared

to the slit area a pressure loss in the lines could not be detected. All pressure gages were calibrated just before being installed.

D. Computations

The dynamic pressure of the tunnel was computed using the readings of static pressure difference and the tunnel calibration curve. The tunnel velocity was computed using the average value of dynamic pressure (13.3 lbs. ft²) although the dynamic pressure was essentially constant.

$$q = 1/2 \rho v^2$$

$$v = \left[\frac{2q}{\rho} \right]^{1/2} = \left[\frac{2 \times 13.3}{.002378} \right]^{1/2} = 106 \text{ ft/sec}$$

The coefficients of lift, drag, and pitching moment were computed as follows:

$$\begin{array}{l} \text{Lift} \\ C_L = \frac{L}{qS} \end{array}$$

$$\begin{array}{l} \text{Pitching Moment} \\ (C_M)_{50} = \frac{M - m}{q S c} \end{array}$$

$$(C_M)_{25} = (C_M)_{50} - 1/4 C_L$$

$$\begin{array}{l} \text{Drag} \\ C_{D_r} = \frac{d}{qS} \end{array}$$

$$C_D = \frac{D}{qS} - C_{D_r}$$

Velocity (v_s) in slit.

$$v_s^2 + 2 \frac{\gamma}{\gamma-1} \frac{p}{\rho} = 2 \frac{\gamma}{\gamma-1} \frac{p_0}{\rho_0}$$

$$v_s = \left[2 \frac{\gamma}{\gamma-1} \frac{p_0}{\rho_0} \left(1 - \frac{p}{p_0} \right) \right]^{1/2}$$

$$\text{but } \frac{p_o}{p_o} = RT_o$$

$$\frac{p p_o}{\rho p_o} = \frac{p}{\rho_o} \frac{\gamma-1}{\gamma}$$

$$v_s = \left[2 \frac{\gamma}{\gamma-1} RT_o \left(1 - \frac{p}{p_o} \frac{\gamma-1}{\gamma} \right) \right]^{1/2}$$

$$v_s = \left\{ \frac{(2)(1.4)(1716)(550)}{1.4 - 1} \left[1 - \left(\frac{14.7}{44.7} \right) \frac{1.4-1}{1.4} \right] \right\}^{1/2} = 1340 \text{ ft/sec}$$

The coefficient (C_Q) was used as a ratio of the volume of air blown out to the volume of air that would be swept out by an outline of the plan form of the wing set at 90° to the air stream.

$$C_Q = \frac{Q}{VS}$$

Since the Rotometer was designed for standard conditions the following correction was made as per instructions supplied with the instrument and C_Q was computed:

$$Q = Q_R \frac{14.7}{p_o} \times \frac{T_o}{530}$$

for $p_o = 44.7$

$$Q = \frac{18.1}{60} \left[\frac{44.7}{14.7} \times \frac{530}{550} \right]^{1/2}$$

Average $Q_R = 18.1$ c.f.m.

$T_o = 550^\circ$ abs

$$Q = 0.517 \text{ cu.ft. sec.}$$

$$C_Q = \frac{.517}{106 \times 0.695} = 0.00702$$

for $p_o = 34.7$

$$Q = \frac{18.7}{60} \left[\frac{34.7}{14.7} \times \frac{530}{549} \right]^{1/2}$$

$$\text{Average } Q_R = 18.7 \text{ c.f.m.}$$

$$T_o = 549$$

$$Q = 0.472$$

$$C_Q = \frac{.472}{106 \times .695} = 0.0064$$

$$\text{for } p_o = 24.7$$

$$Q = \frac{22.0}{60} \left[\frac{24.7}{14.7} \times \frac{530}{548} \right]^{1/2}$$

$$\text{Average } Q_R = 22.0$$

$$T_o = 548$$

$$Q = 0.467$$

$$C_Q = \frac{.467}{106 \times .695} = 0.00634$$

III. RESULTS AND CONCLUSIONS

A. Results

A comparison of results is presented in the following tabular forms.

The first table presents the maximum lift coefficient and the corresponding drag coefficient for each of the best runs. The increment of maximum lift and drag coefficient (ΔC_L , ΔC_D) are the differences between the lift and drag coefficients for the unflapped wing at $C_Q = 0$ and the lift and drag coefficients for the flapped and or blowing wing.

TABLE I

Wing Configuration				α	at $C_{L_{max}}$				% increase		
Nose	Trailing	P_0	C_Q		C_L	C_D	ΔC_L	ΔC_D	C_L	C_D	α
0	0	0	0	10	.808	.166	0	0	0	0	0
0	60	0	0	6	1.68	.40	0.87	.23	107.5	139	-.40
0	60	44.7	0.0070	10	1.94	.45	1.13	.28	140.0	167	0
150	0	0	0	15	1.09	.210	.28	.044	33.4	26.5	50
0	0	44.7	0.0070	16	1.28	.280	.47	.116	58.2	70.0	60
150	60		0	9	1.90	.430	.09	.264	11.1	159.0	-10.0
150	60	44.7	.0070	12	2.18	.480	1.37	.314	170.0	189.0	20.0
120	60	44.7	.0070	24	2.35	.550	1.54	.384	190.0	231.0	140.0

It is noted that the percent drag increase is greater than the percent lift increase. However, at the higher lift configurations the greater drag increment is due to the flattening of the drag curve near the stall and in particular, where blowing was used, to the great increase in angle of attack.

A more favorable comparison is presented in the second table. Here the increase of the lift and drag coefficients and the angle of attack due to blowing is shown for each configuration of flaps. It is noted that boundary layer control by blowing increases the lift coefficient of all the wing configurations tested.

TABLE II

Wing Configuration					at C_{Lmax}				% increase		
Nose	Trailing	p_0	C_Q	α	C_L	C_D	ΔC_L	ΔC_D	C_L	C_D	α
0	0	0	0	10	.808	.166	0	0	0	0	0
0	0	24.7	.0063	15	1.08	.225	.27	.059	33.4	35.6	50
0	0	34.7	.0064	16	1.20	.25	.39	.08	48.3	48.2	60
0	0	44.7	.0070	16	1.28	.26	.47	.09	58.2	54.2	60
0	60°	0	0	6	1.68	.40	0	0	0	0	0
0	60°	44.7	.0070	10	1.94	.45	.26	.05	15.5	12.5	67
150°	60°	0	0	9	1.90	.430	0	0	0	0	0
150°	60	44.7	.0070	12	2.18	.480	.28	.050	14.7	11.6	33

B. Conclusions

The data indicates that:

1. The slope of the lift curve was essentially constant for all configurations of the wing tested.
2. There is an appreciable increase of angle of attack and lift when the nose flap alone is used.
3. Trailing edge split flaps increase the lift of this wing as would be expected.

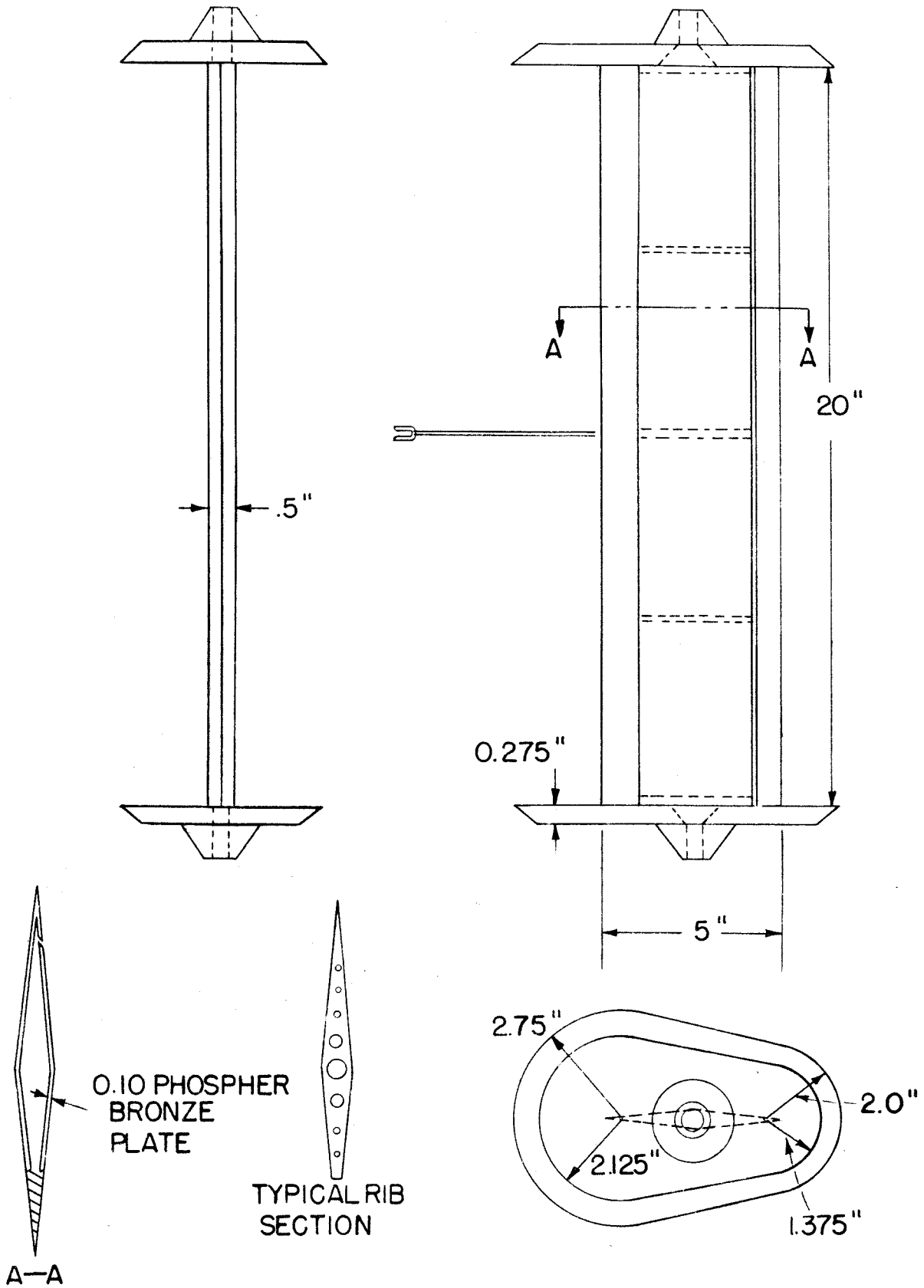
4. The combination of nose and trailing edge flaps on the wing, while giving a great increase in lift, caused the wing to stall at about the same angle of attack as the stall angle for the basic wing. The addition of the jet boundary layer control to the flapped wing increased the angle of attack appreciably and thus increased the lift.

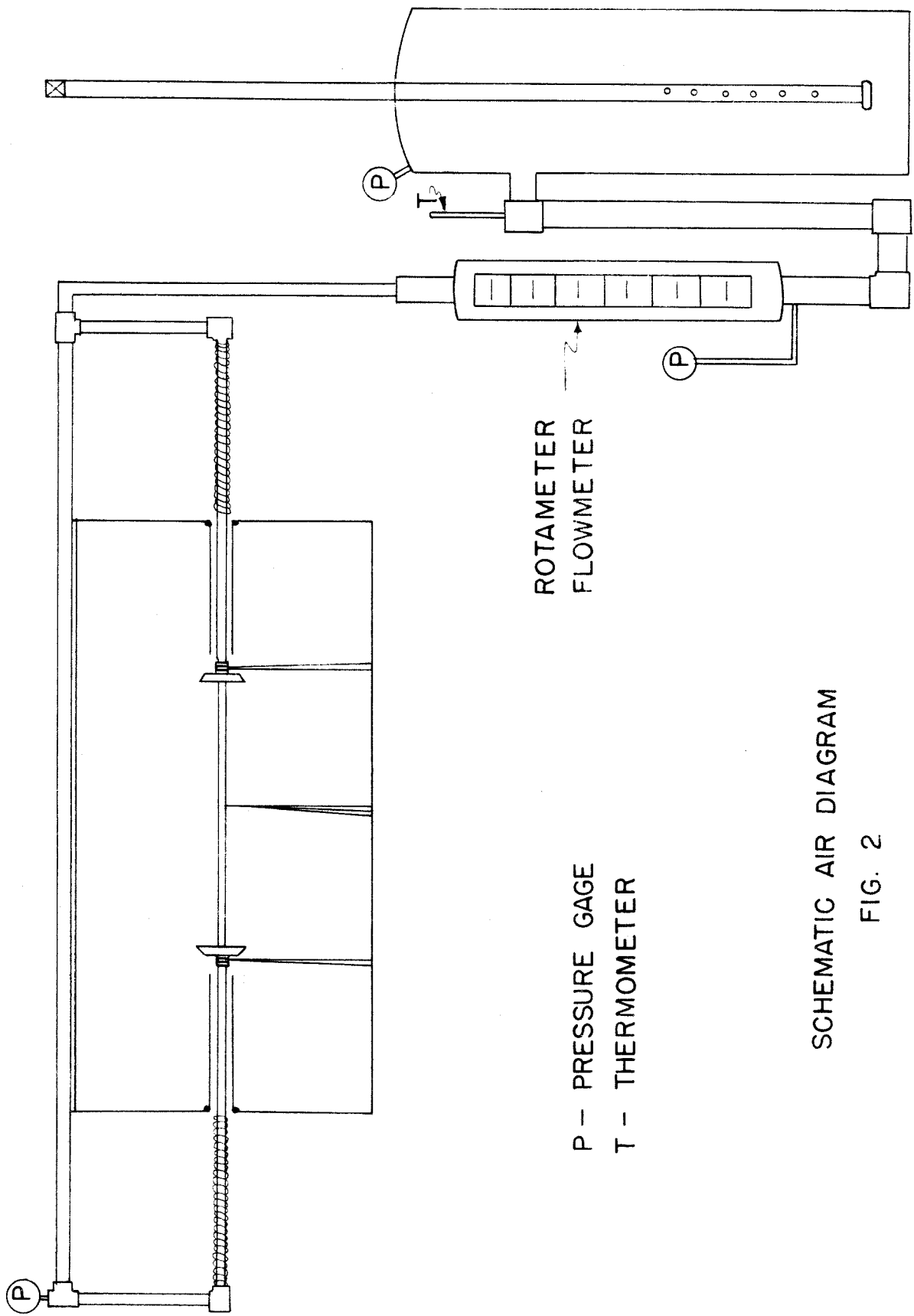
5. The boundary layer control by blowing improves the wing characteristics sufficiently to warrant much further study. It should be noted that the model was tested with the jet slit located at the 15 percent wing chord line and at a coefficient of discharge of air of 0.0070. It is suggested therefore, that further tests be made with the current model. The optimum position of the jet slit and the most practicable value of C_Q could be investigated.

REFERENCES

1. Schwier, W. - Lift Increase by Blowing out Air: Tests on Airfoil of 12% Thickness Using Various Types of Flap. GER No. 219.
2. Schwier, W. - Lift Increase Produced by Blowing a Wing of a Profile Thickness of 9% Equipt with a Slat and a Slotted Flap. No. F-TS-645-RE.
3. Kruger, W. - The Nose Flap as a Means for Increasing the Maximum Lift of High-Speed Aeroplanes. CGD 532.
4. Smith, A.M.O. - A Preliminary Study of the Problem of Boundary Layer Control.
5. Kleber, J.A., Schwarzbach, J.M. - Wind Tunnel Tests of Flap and Aileron-Flap Combination. Curtiss-Wright Corp. Report No. 9367.
6. Smith, A.M.O., Roberts, H.E. - The Jet Airplane Utilizing Boundary Layer Air for Propulsion. Douglas Aircraft Co., Inc. Report.
7. Fischer & Porter Company - Theory of the Rotameter, Catalog Section 98-Y.
8. Weske, J.R.- Reduction of Skin Friction on a Flat Plate. JRAS 1939.
9. Richardson, E.G.- Manipulation of Boundary Layer. JRAS 1938.
10. Freeman, H.B., - Boundary Layer Control Tests. NACA T.N. 1007.

FIG. 1
MODEL II





SCHEMATIC AIR DIAGRAM

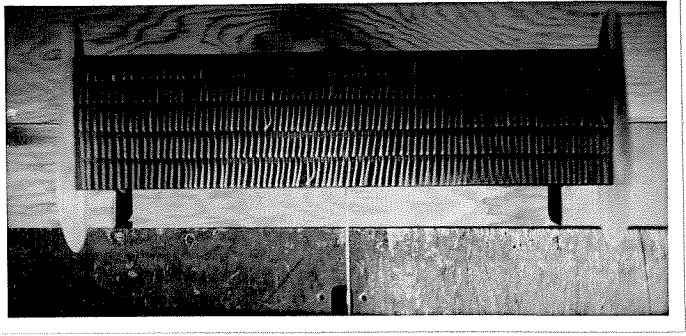
FIG. 2

Tuft Survey

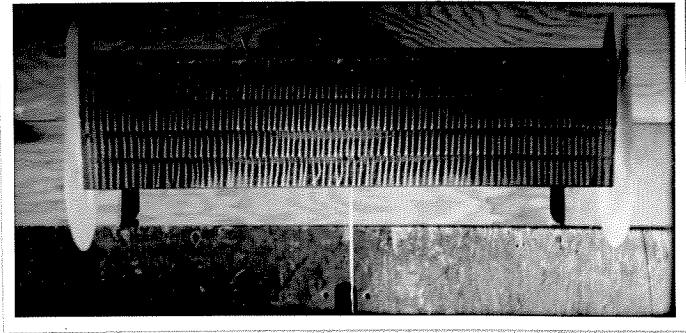
Fig. 3

No Flap
 $q = 13.3 \text{ lbs/ft}^2$

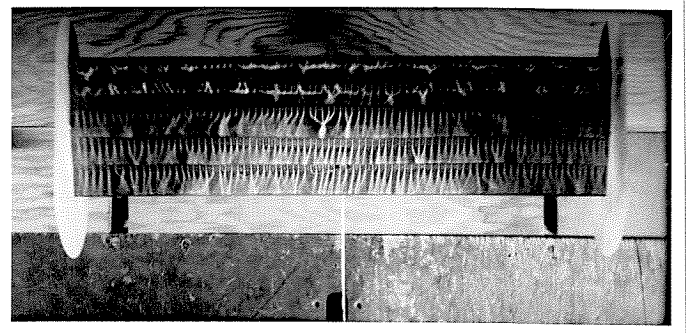
Angle of attack
 $\alpha = 0$



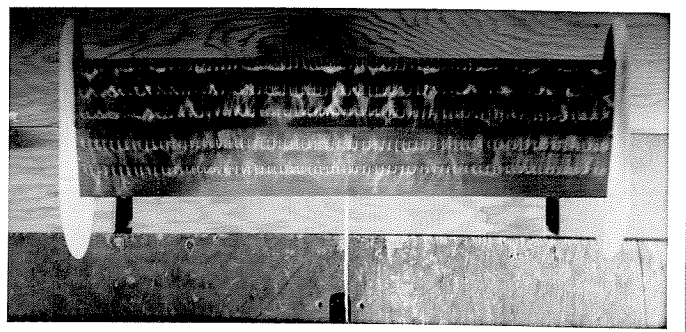
$\alpha = 5^\circ$



$\alpha = 8^\circ$



$\alpha = 12^\circ$



Tuft Survey

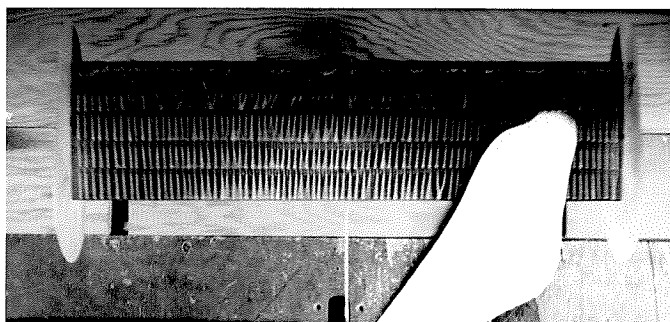
Fig. 4

60° Tail Flaps

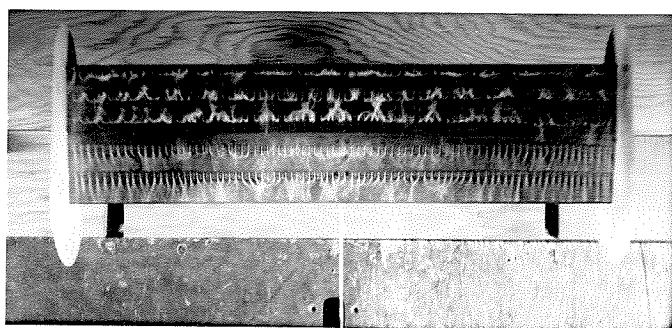
$q = 13.3 \text{ lbs/ft}^2$

Angle of Attack

$\alpha = 0^\circ$



$\alpha = 5^\circ$



Tuft Survey

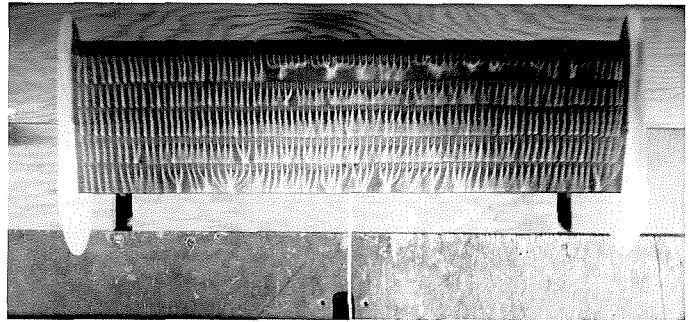
Fig. 5

150° Nose Flap

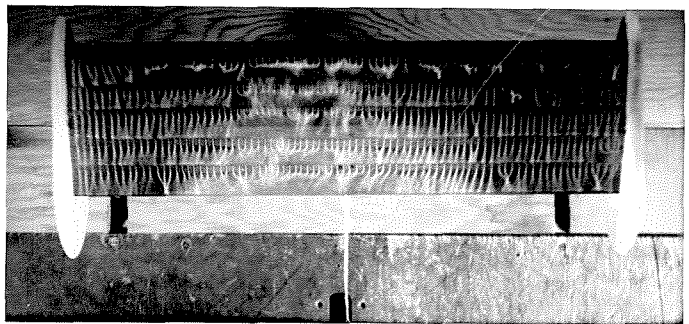
$q = 13.3 \text{ lbs/ft}^2$

Angle of attack

$$\alpha = 11^\circ$$



$$\alpha = 13^\circ$$



$$\alpha = 15^\circ$$



Tuft Survey

Fig. 6

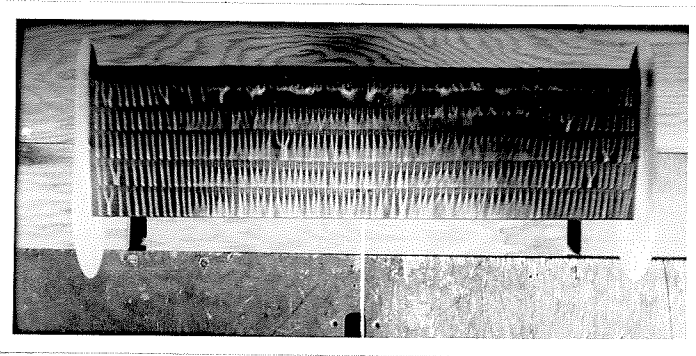
60° Tail Flaps

150° Nose Flaps

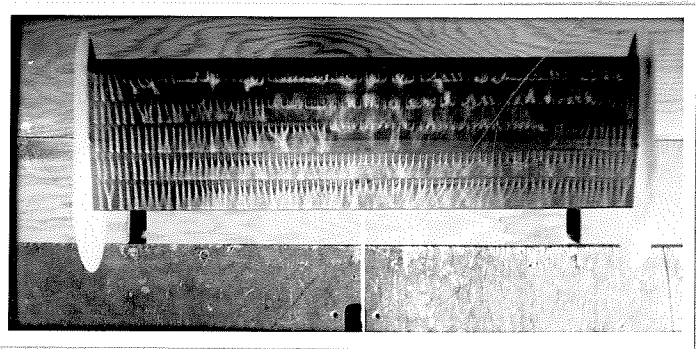
$q = 13.3 \text{ lbs/ft}^2$

Angle of Attack

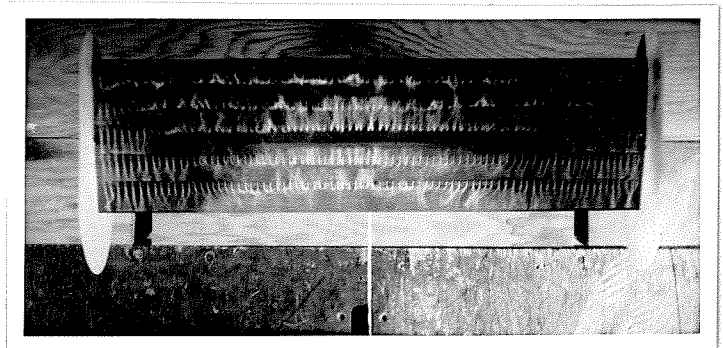
$$\alpha = 6^\circ$$



$$\alpha = 8^\circ$$



$$\alpha = 10^\circ$$



3.0

2.0

1.0

INCHES

0

-1.0

FIG. 7

$\alpha = 6^\circ$

LINES OF CONSTANT $\frac{\Delta H}{q}$

0.1

0.2

0.4

0.6

α

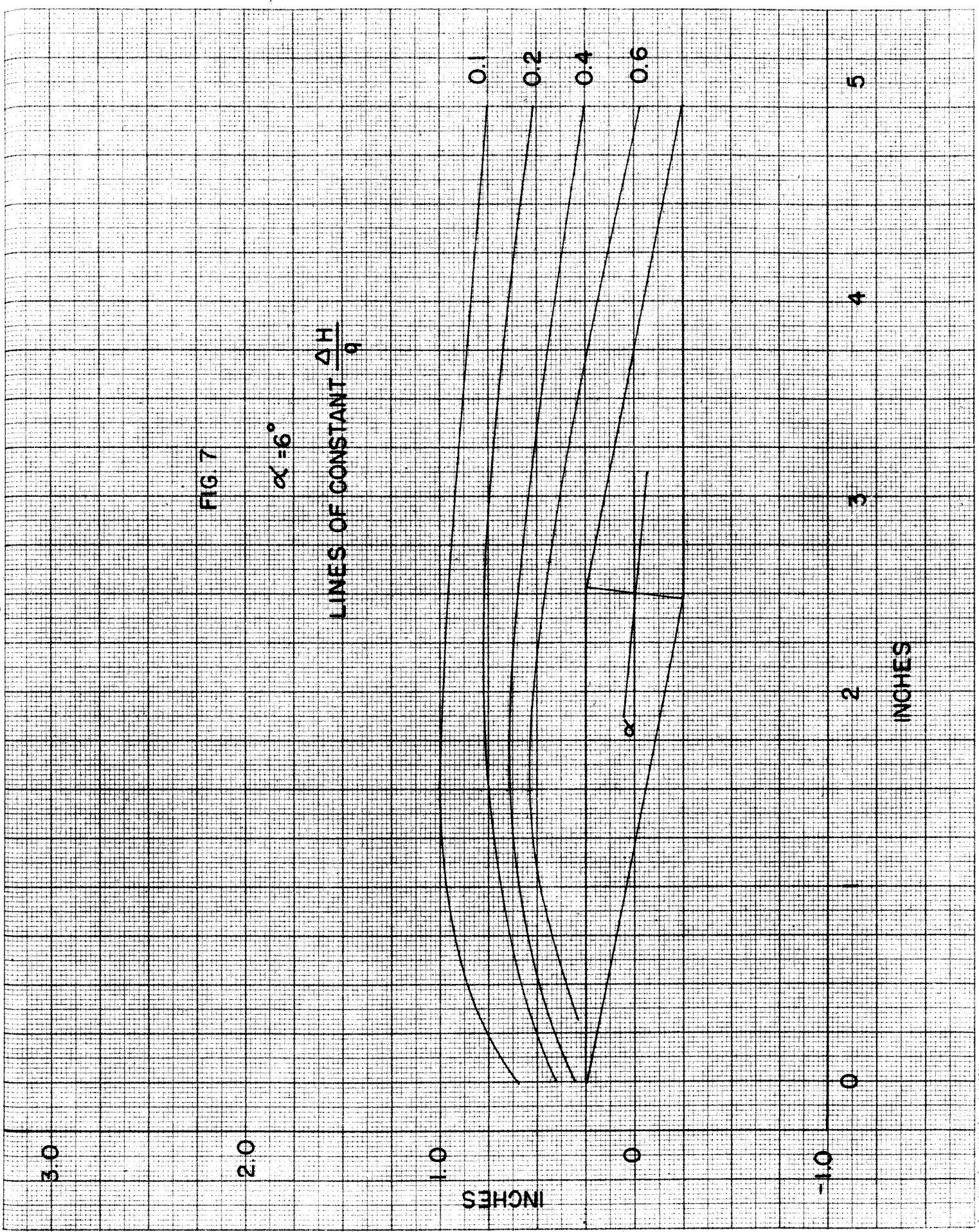
2

3

4

5

INCHES



3.0

2.0

1.0

0

-1.0

INCHES

FIG. 8

$\alpha = 10^\circ$

LINES OF CONSTANT $\frac{\Delta H}{q}$

0.2

0.4

0.6

1.5

1.45

α

30

40

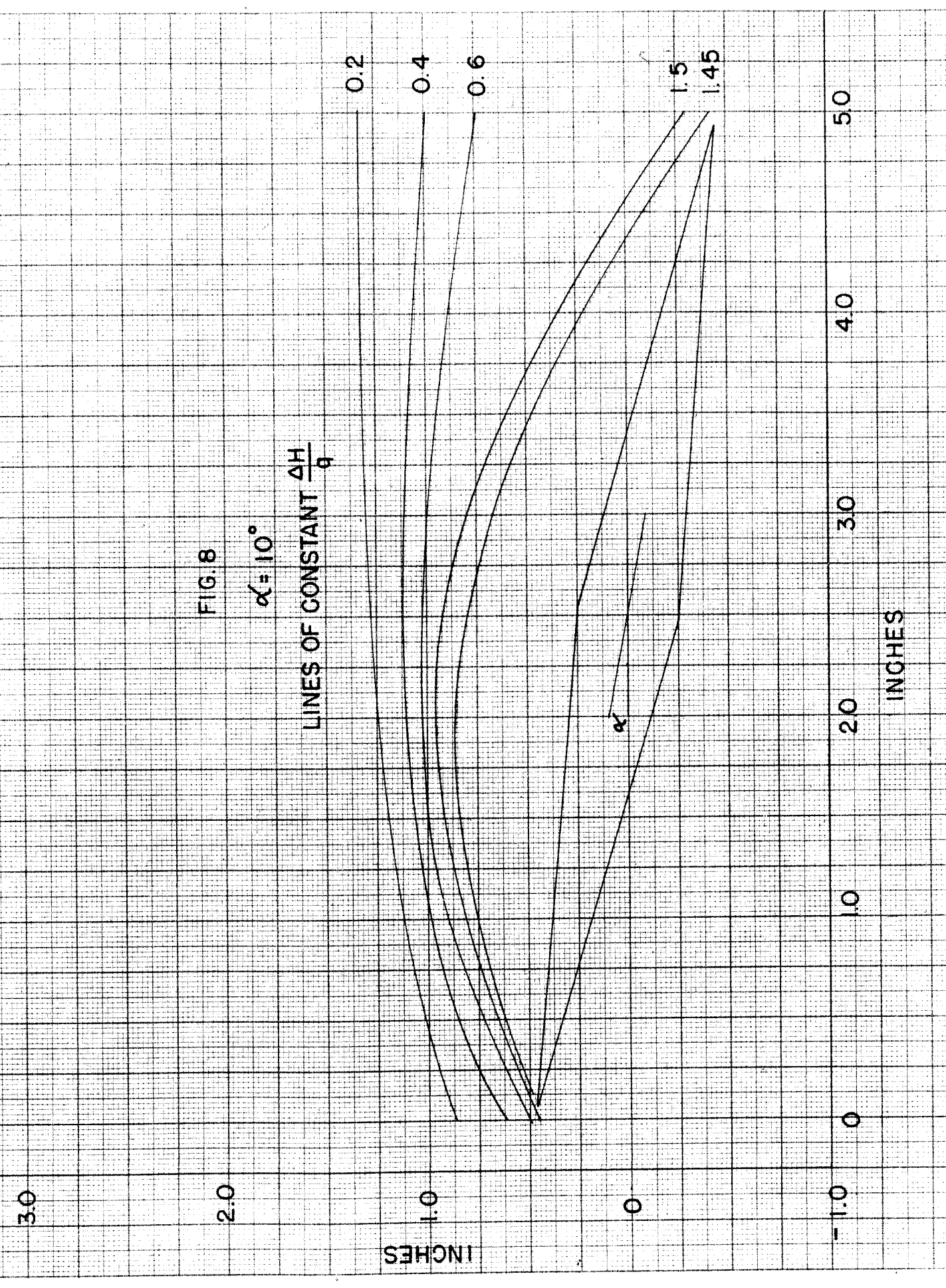
50

INCHES

1.0

0

-1.0



3.0

2.0

INCHES

1.0

0

-1.0

FIG. 9

$$\alpha = 14^\circ$$

LINES OF CONSTANT $\frac{\Delta H}{q}$

0.2

0.4

0.6

1.6

1.8

1.85

3.0

2.0

1.0

0

-1.0

5.0

INCHES

4.0

3.0

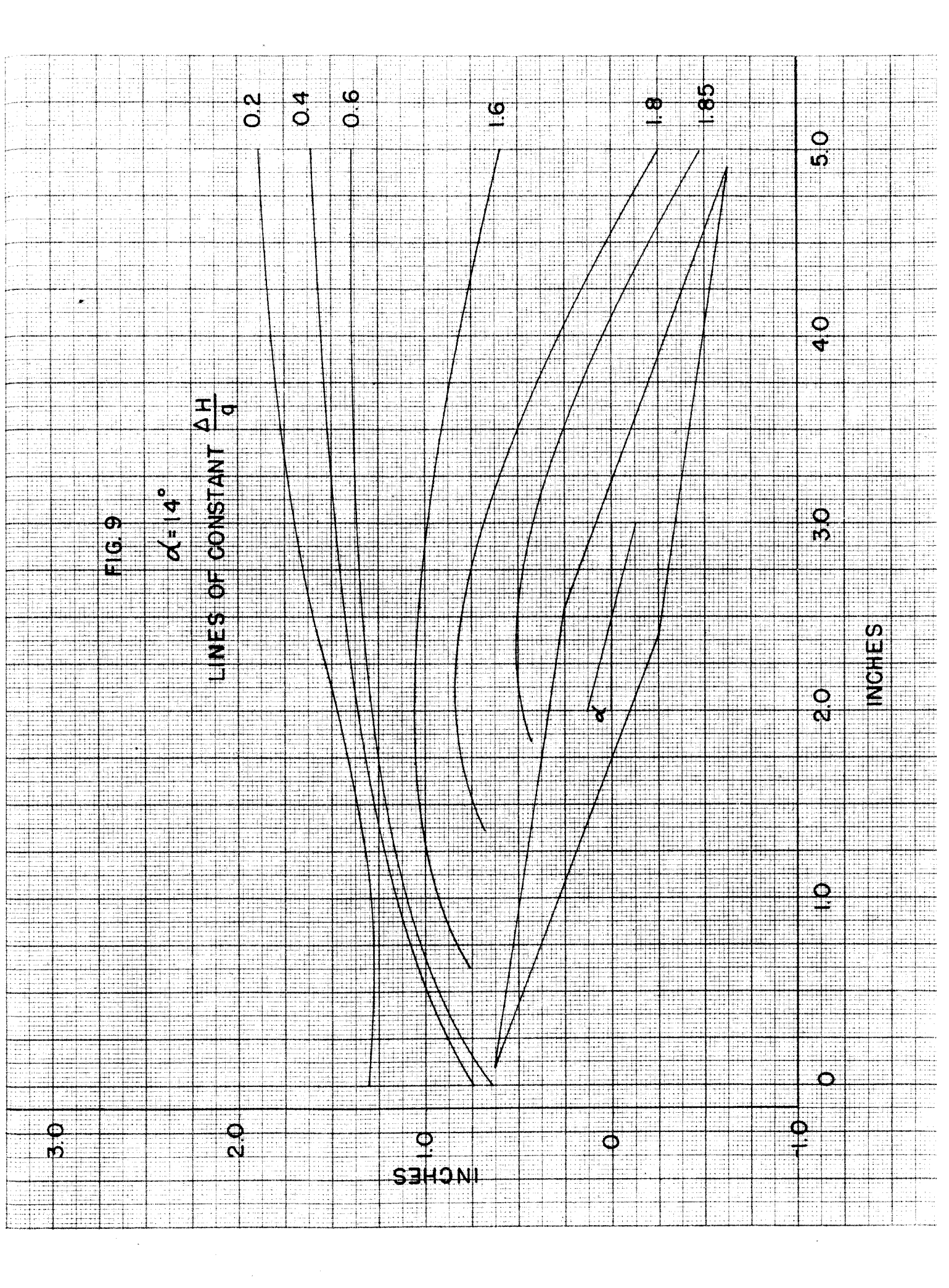
2.0

1.0

0

-1.0

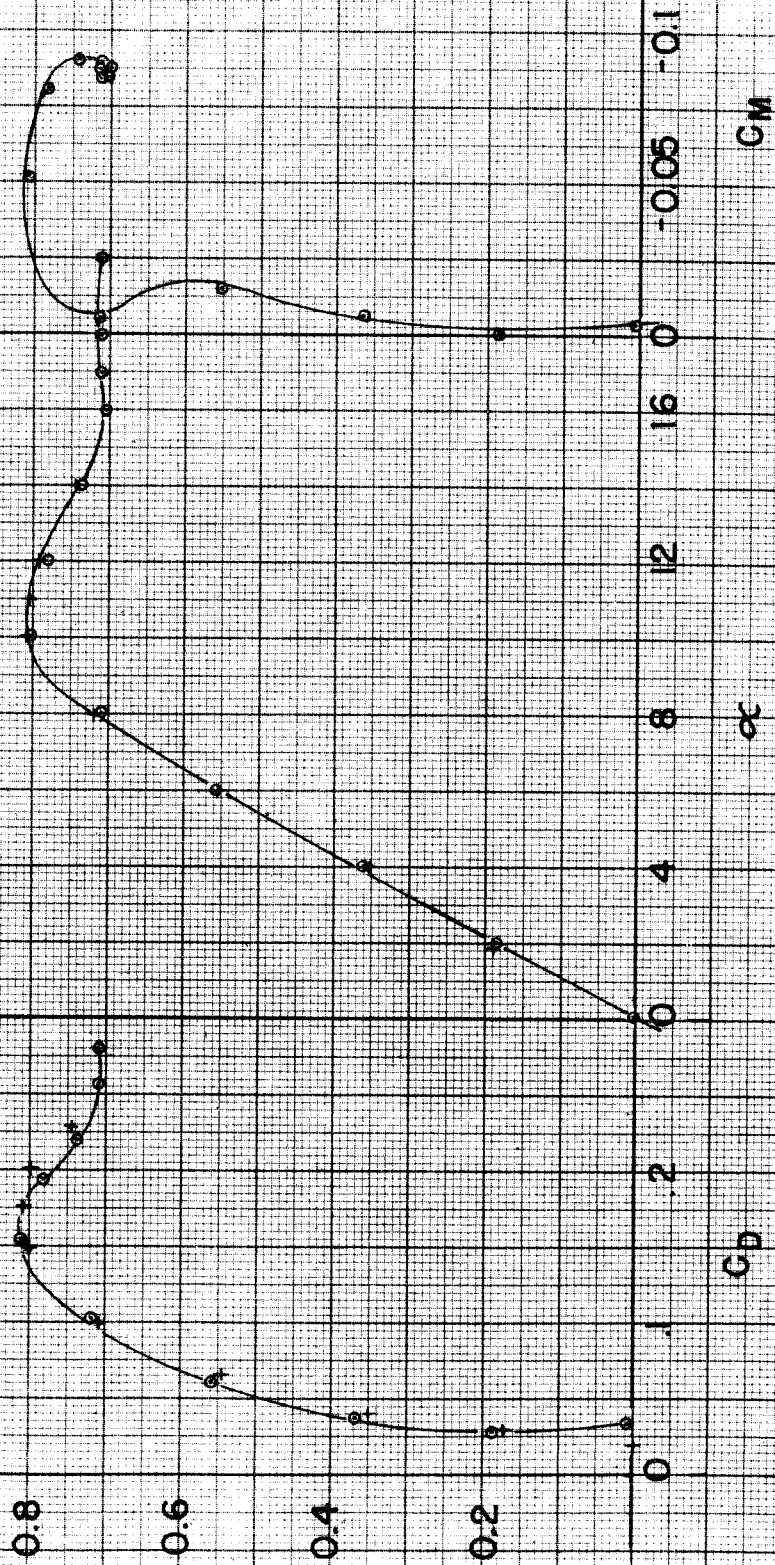
5.0



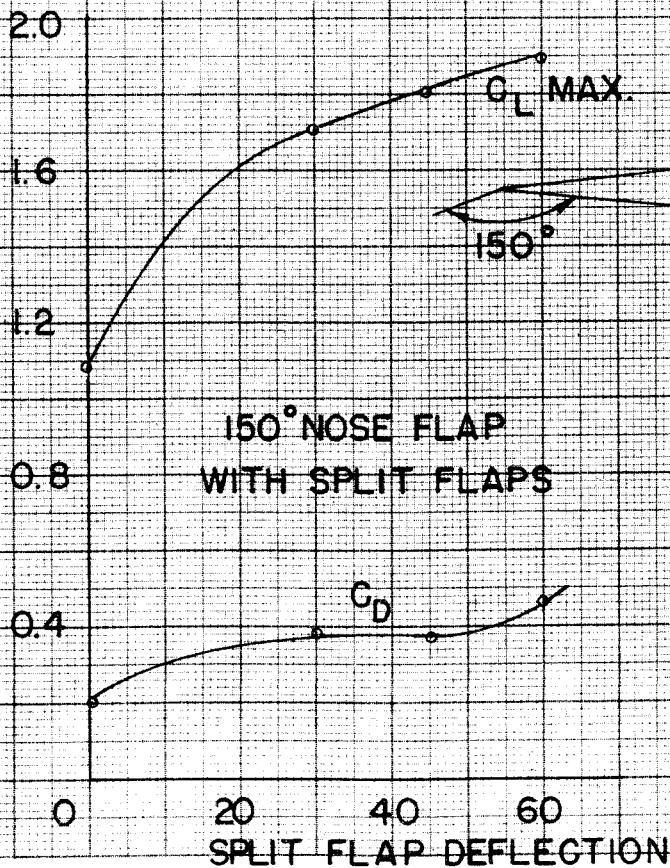
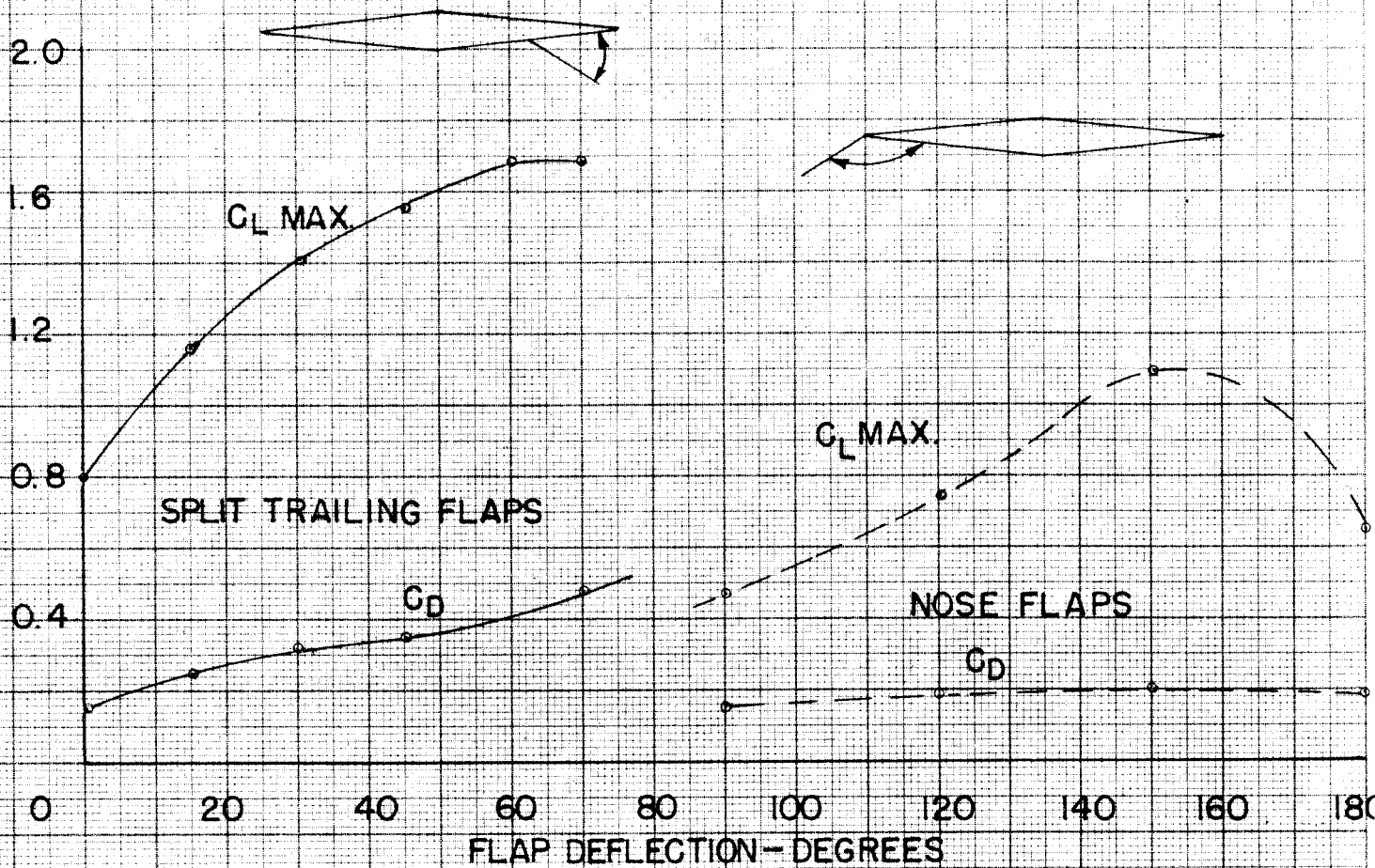
NO FLAPS

○ POSITIVE INCREMENTS OF α "
+ " " " " "
+ NEGATIVE " " " " "

MOD. I FIG. 10



MOD I FIG. 11



MOD I FIG 12

MOD II FIG. 13

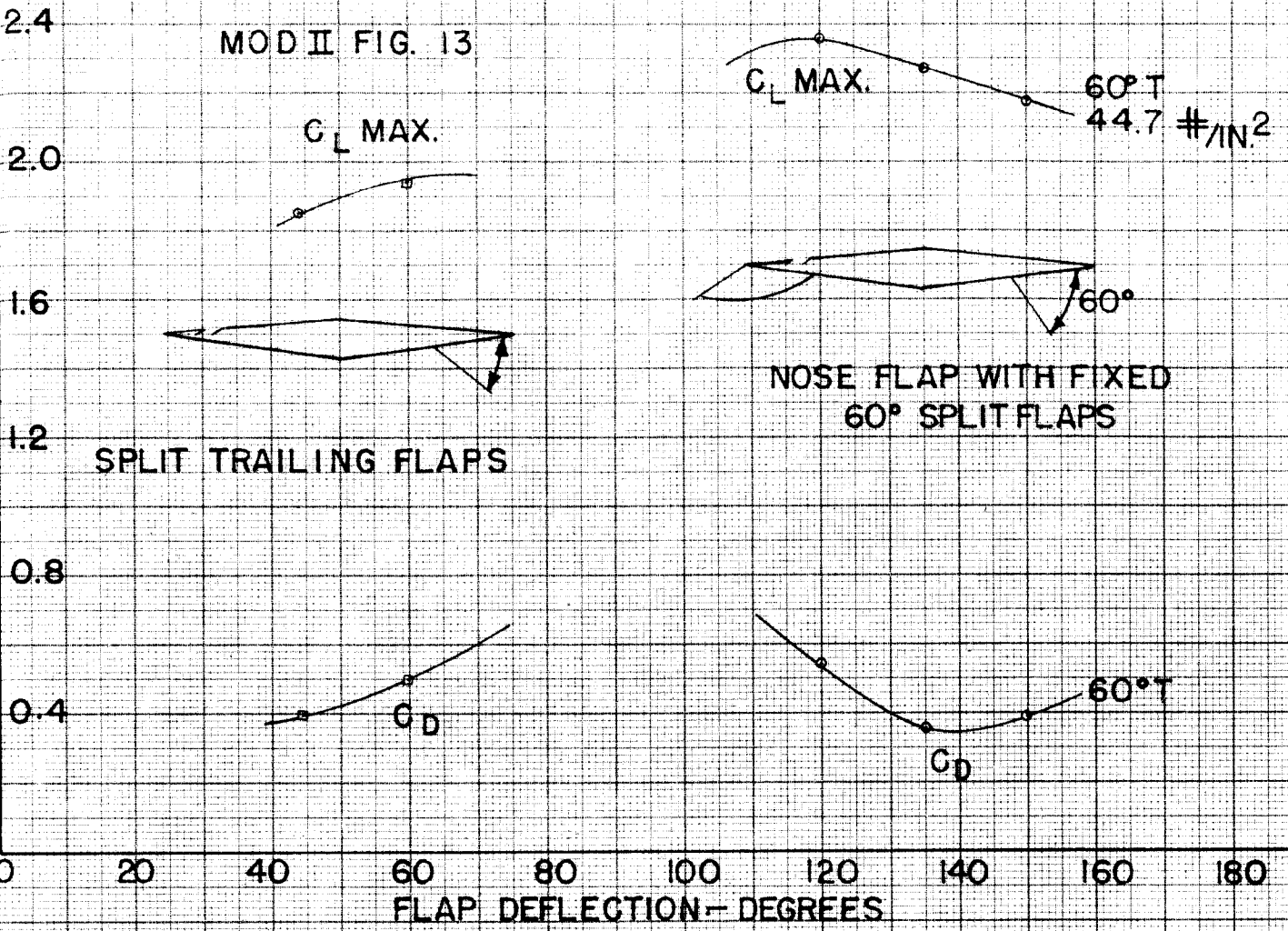
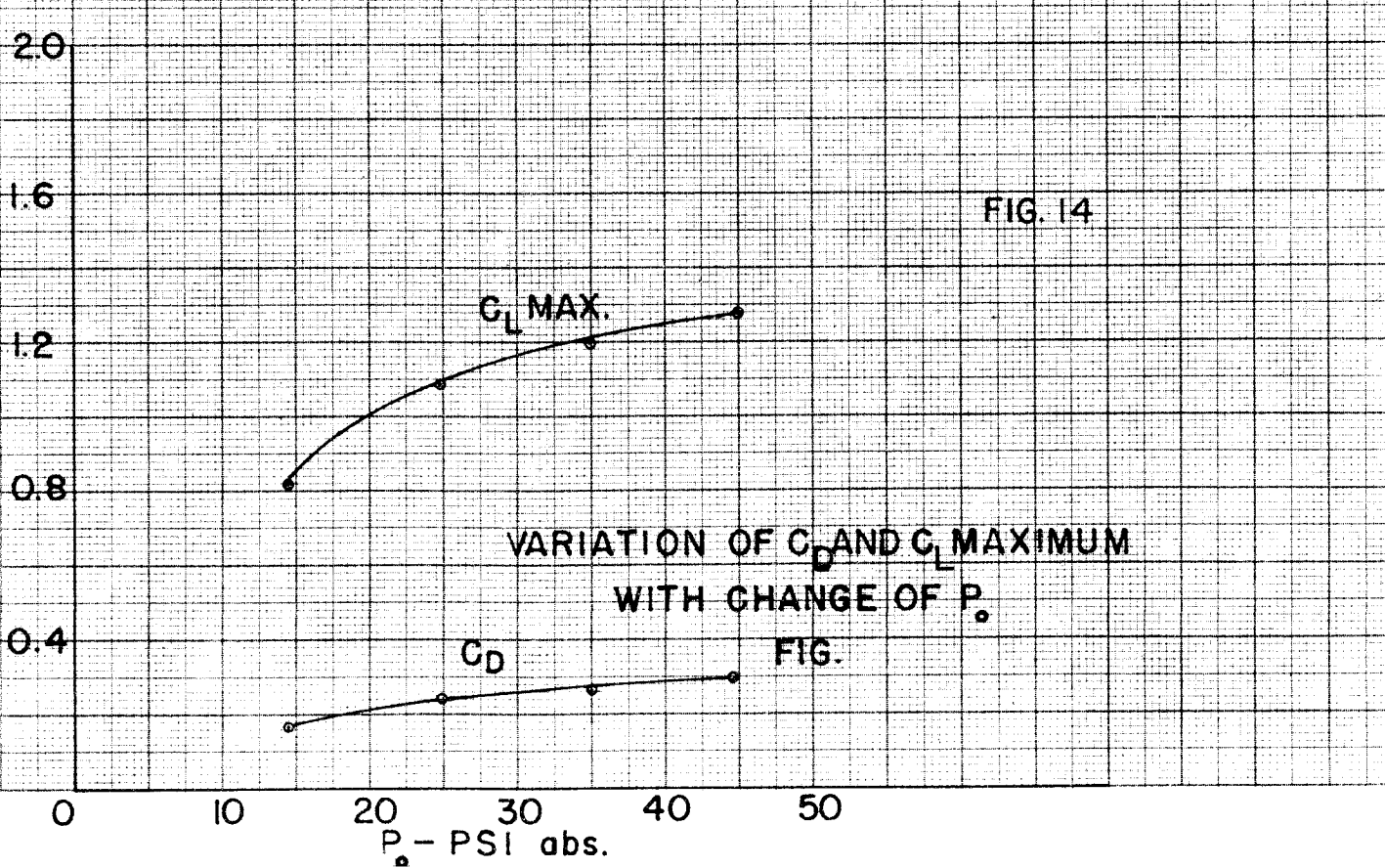


FIG. 14



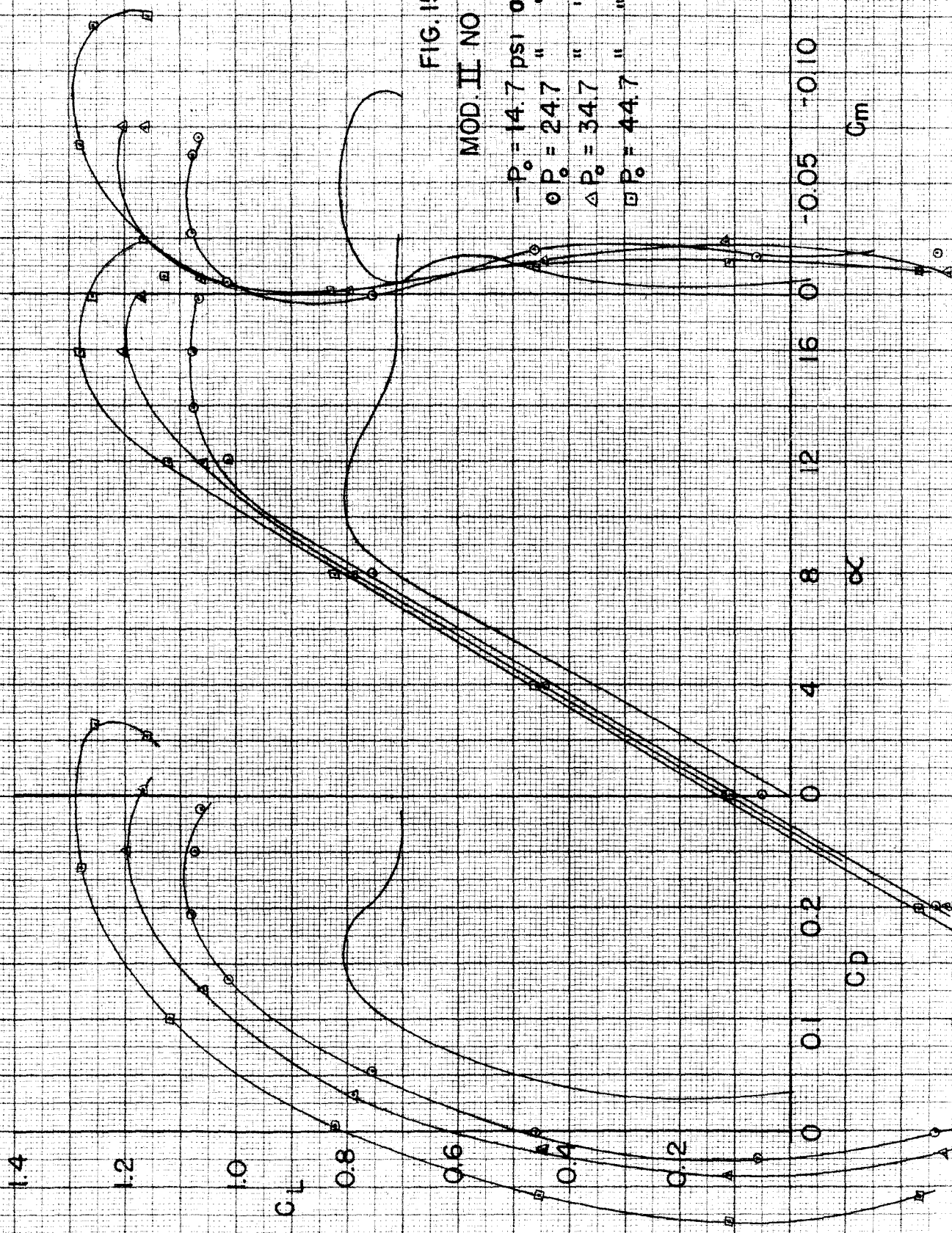


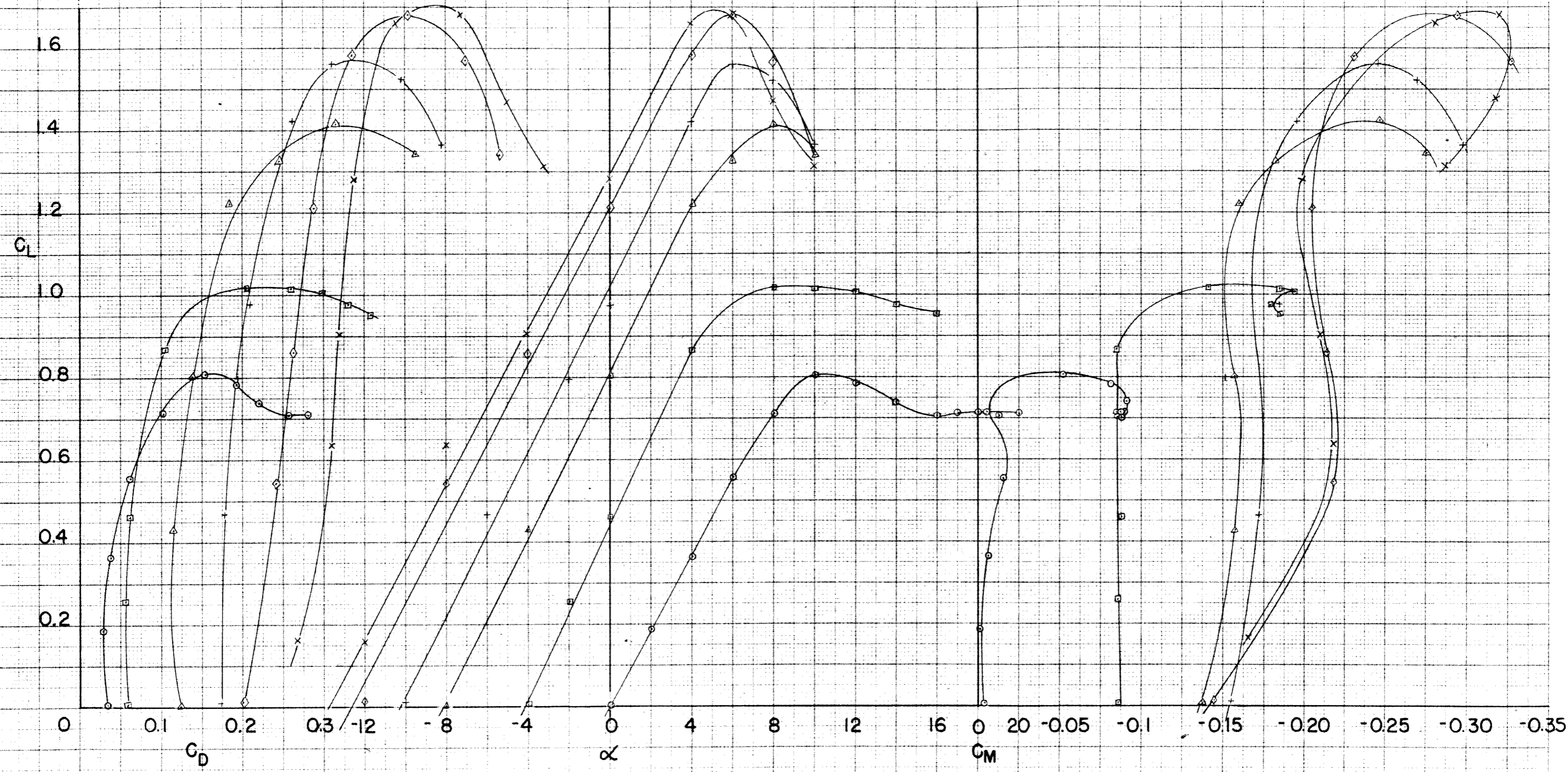
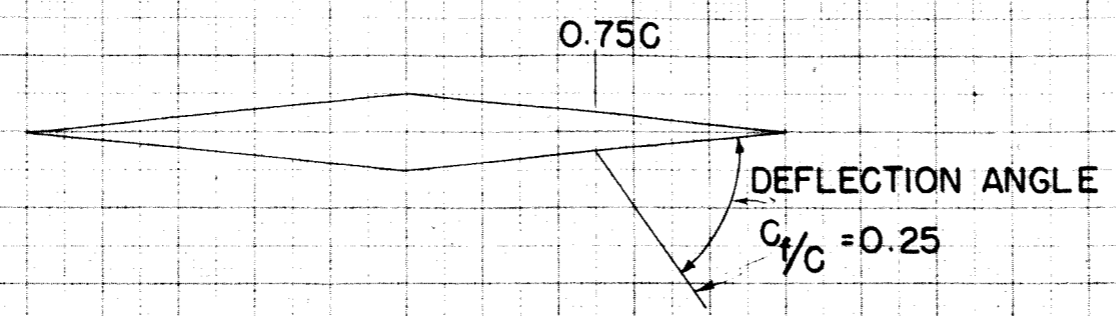
FIG. 15

MOD. II NO FLAPS

-P ₀ = 14.7 psi	obs.	C _Q = 0
○ P ₀ = 24.7 "	"	C _Q = 0.00634
△ P ₀ = 34.7 "	"	C _Q = 0.0064
◻ P ₀ = 44.7 "	"	C _Q = 0.00702

MOD I
SPLIT FLAPS - FIG. 16

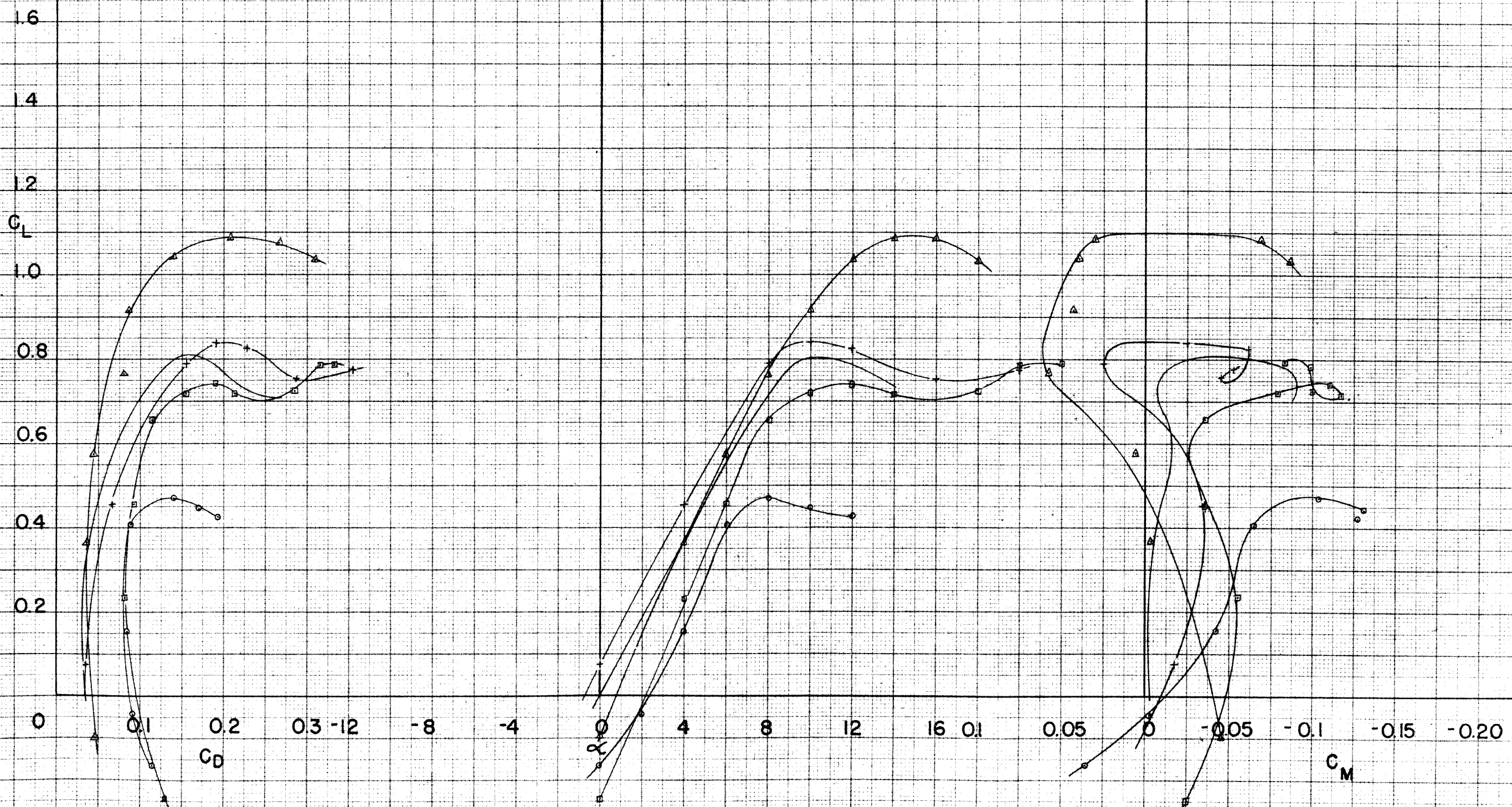
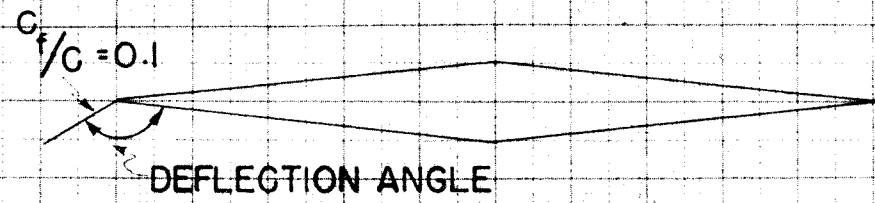
- NO FLAP DEFLECTION
- 15°
- △ 30°
- + 45°
- ◇ 60°
- × 70°



MOD I
NOSE FLAPS-FIG. 17

— NO FLAP DEFLECTION

- 90° " "
- 120° " "
- △ 150° " "
- + 180° " "

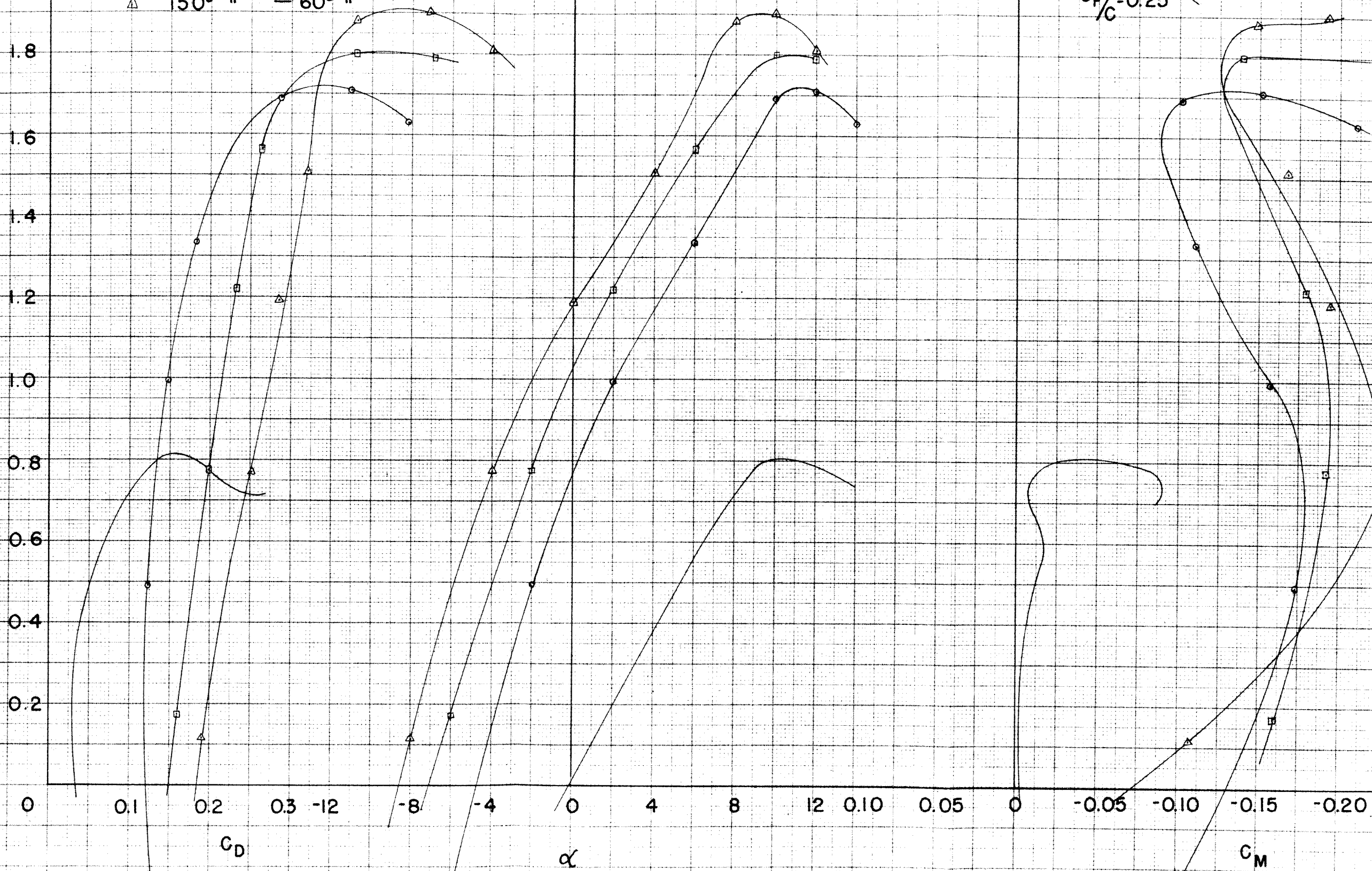
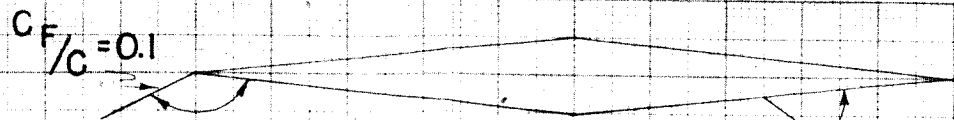


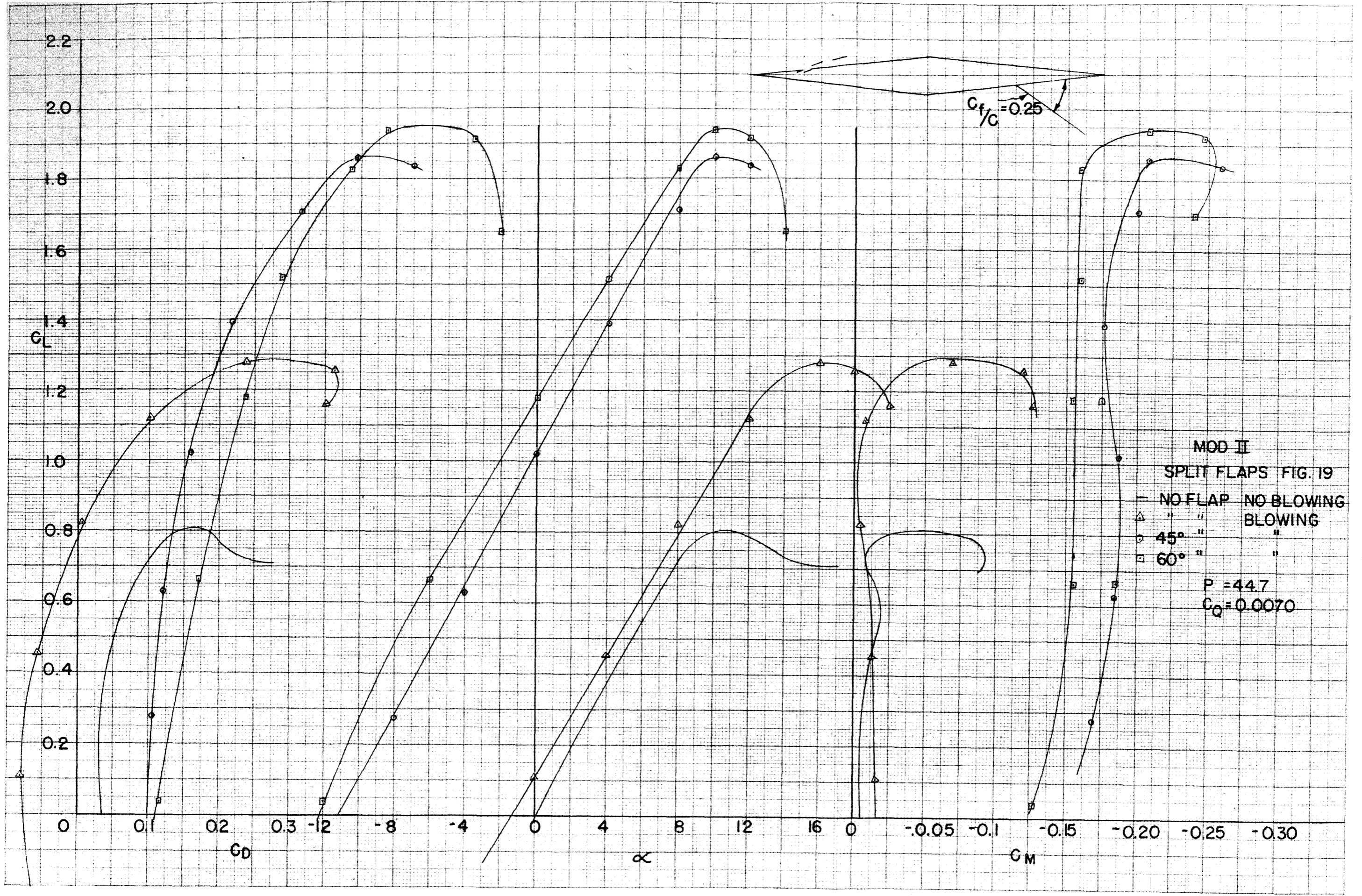
MOD I
COMBINED FLAPS—FIG. 18

- NO FLAP DEFLECTION
- 150° NOSE — 30° TAIL
- 150° " — 45° "
- △ 150° " — 60° "

$C_F/C = 0.1$

$C_F/C = 0.25$





MOD II
 COMBINE FLAPS FIG. 20
 - NO FLAP

- 150° NOSE 60° TAIL
- △ 135° " 60° "
- 120° " 60° "

$P_0 = 44.7$
 $C_Q = 0.0070$

